Thermochimica Acta, 163 (1990) 225-232
Elsevier Science Publishers B.V., Amsterdam - Printed in The Netherlands

THERMAL AND DIELECTRIC PROPERTIES OF MANGANESE SQUARATE CLATHRATE COMPOUND*

Y. MIYAZAKI and T. MATSUO

Department of Chemistry and Microcalorimetry Research Center, Faculty of Science, Osaka University, Toyonaka, Osaka 560 (Japan)

SUMMARY

The heat capacity and complex dielectric permittivity of the manganese squarate clathrate compound $(MnC_4O_4 \cdot 2H_2O)_3(CH_3COOH)_{0.75}(H_2O)_{0.19}$ were measured in the temperature ranges from 12 to 300 K and from 20 to 250 K, respectively. Two dielectric dispersions were found, indicating that there are two different motional modes of the guest molecules. A higher order phase transition was found at 60.7 K. The static dielectric permittivity of the compound had a peak at ∿60 K in agreement with the calorimetric result and suggested an order-disorder mechanism for the phase transition.

INTRODUCTION

Recently a new type of clathrate compounds $(MC_4O_4 \cdot 2H_2O)_3 \cdot CH_3COOH \cdot H_2O$ where M is Ni, Zn, or Mn was synthesized and characterized (refs. 1,2). The X-ray structural studies showed that the nickel and zinc compounds crystallize in the cubic space group Pn3n and that the manganese and zinc compounds synthesized in high ionic strength solution crystallize in the triclinic space group $P\bar{1}$. Every compound has cage-like cavities in which a pair of acetic acid and water molecules is trapped. The guest molecules could not be located in the X-ray works probably because of the large cavity size that allowed them a large motional amplitude. At low temperatures, the substances are expected to undergo either a phase transition or a kinetic anomaly. We measured the heat capacity and complex dielectric permittivity of the manganese squarate clathrate compound over a wide range of temperature.

EXPERIMENTAL

The sample was synthesized following the method described in ref. 2. The result of elemental analysis of the sample was Mn: 25.09 %, C: 24.69 %, H: 2.41 %, O: 47.81 %; the theoretical value calculated for the formula $(MnC_4O_4 \cdot 2H_2O)_3 \cdot CH_3COOH \cdot H_2O$ is Mn: 23.99 %, C: 24.47 %, H: 2.64 %, O: 48.90 %. The occupation fractions of the guest molecules of the sample calculated from

*Contribution No. 12 from the Microcalorimetry Research Center.

0040-6031/90/$03.50

the analytical result were CH_3COOH: 0.75 ± 0.03 and H_2O: 0.19 ± 0.06. This does not agree with stoichiometry of the guest molecules reported previously (ref. 2).

Heat capacity measurement was carried out with an adiabatic low-temperature calorimeter for small samples (ref. 3). Modification of the calorimeter was made in several aspects for better precision and shorter experimental time. First, the platinum resistance thermometer (Minco Products, 1060, U.S.A., nominal 100 Ω) was replaced by a rhodium-iron alloy resistance thermometer (Cryogenic Calibrations Ltd., 1550, Great Britain, nominal 27 Ω). This increased the resolution of the thermometry at lower temperatures (from ±1.5 mK to ±0.3 mK at 15 K). Thus the temperature measurement could be performed more accurately and precisely at low temperatures. Secondly, the Teflon-coated Chromel-Constantan thermocouples for the temperature transfer and adiabatic control were changed to Formvar-coated Chromel-Constantan thermocouples. This reduced the heat capacity of the thermocouple wires. At the same time, the number of the thermocouples for temperature transfer was increased from a pair to three pairs. By these modifications, the thermal relaxation time became remarkably shorter than before (from ∿30 min. to ∿8 min. at 100 K) and the temperature transfer could be made more precisely than before (from ±0.12 mK to ±0.06 mK at 80 K). Thus the experimental time was notably shortened and the temperature of the sample could be measured with higher resolution. Actually the precision of the heat capacity measurement was within 0.1 % above 30 K. By the use of the improved calorimeter, the heat capacity of the compound was measured from 12 to 300 K with the sample amount of 0.9646 g (1.467×10^{-3} mol).

The complex dielectric permittivity was measured in the temperature range between 20 and 250 K with a capacitance bridge (General Radio Co., 1615-A, U.S.A.) at seven frequencies between 100 Hz and 10 kHz and a multi-frequency LCR meter (Yokogawa-Hewlett-Packard Ltd., 4275A, Japan) at seven frequencies between 10 kHz and 1 MHz by the two-terminal method. The cryostat was described elsewhere (ref. 4). The sample was powdered and pressed to form a disk of 13.15 mm in diameter and 0.863 mm in thickness. Thin gold foil electrodes, 0.05 mm in thickness, were attached to both faces of the disk with a small amount of Apiezon N (Apiezon Products Ltd., Great Britain).

RESULTS AND DISCUSSION

The molar heat capacity data of the manganese squarate clathrate compound are listed in Table 1 and plotted against temperature in Fig. 1, where the composition $(MnC_4O_4 \cdot 2H_2O)_3(CH_3COOH)_{0.75}(H_2O)_{0.19}$ determined from the analytical result was adopted as the molar basis. A heat capacity anomaly was found at 60.7 K. The temperature dependence of the heat capacity anomaly (absence of a

TABLE 1

Molar heat capacity of $(MnC_4O_4 \cdot 2H_2O)_3(CH_3COOH)_{0.75}(H_2O)_{0.19}$.

T/K	C_p/J K^{-1}mol^{-1}	T/K	C_p/J K^{-1}mol^{-1}	T/K	C_p/J K^{-1}mol^{-1}	T/K	C_p/J K^{-1}mol^{-1}
188.22	525.9	105.00	345.1	31.36	80.65	57.86	210.3
190.31	529.7	106.97	350.1	32.37	85.55	59.21	218.1
192.40	533.2	108.94	355.4	33.36	90.63	64.39	229.7
194.49	537.0	110.92	360.3	34.35	95.47	65.73	233.4
196.60	540.6	112.89	365.0			67.07	237.4
198.70	544.5	114.87	369.9			68.42	241.1
200.82	548.2	116.85	374.9	11.85	11.42		
202.94	552.1	118.84	379.5	12.78	13.66		
205.06	555.6	120.83	384.5	13.72	16.07	55.54	196.5
207.20	558.9	122.82	389.6	14.67	18.54	56.58	203.0
209.33	562.6	124.82	394.0	15.61	21.28	57.62	208.0
211.47	566.7	126.83	398.6	16.56	24.15	58.66	215.7
213.62	569.9	128.84	403.3	17.50	27.04	59.70	218.9
215.78	574.5	130.85	407.7	18.44	30.10	60.75	224.3
217.94	577.9	132.87	412.7	19.38	33.27	61.80	224.1
220.10	582.0	134.90	417.0	20.31	36.63	63.38	227.0
222.28	585.7	136.94	421.8	21.24	39.91	65.47	232.2
224.46	589.6	138.98	426.1	22.20	43.39	67.53	238.4
226.64	593.4	141.02	430.7	23.20	46.99	69.57	244.8
228.83	597.2	143.08	435.4	24.22	50.60	71.59	250.8
231.03	601.0	145.14	440.0	25.25	54.55	73.60	257.3
233.23	604.9	147.21	444.4	26.29	58.77	75.46	262.9
235.44	608.6	149.29	448.6	27.33	62.97	77.19	268.2
237.66	612.4	151.38	452.8	28.37	67.40	78.91	272.6
239.88	616.4	153.47	457.3	29.40	72.04	80.33	278.2
242.11	619.6	155.57	461.3	30.42	76.32	82.34	283.4
244.35	623.0	157.68	465.8	31.44	81.37		
246.59	626.3	159.80	470.5	32.44	86.38		
248.84	630.6	161.93	474.9	33.53	91.82	47.82	157.2
251.09	633.5	164.07	479.0	34.69	97.88	48.82	165.3
253.35	637.3	166.21	483.7			49.83	169.8
255.62	640.8	168.36	487.8			50.83	174.5
257.89	644.2	170.53	491.7	13.68	15.87	51.84	180.0
260.17	647.7	172.70	495.9	15.06	19.59	52.86	184.9
262.46	651.1	174.88	499.2	16.32	23.43	53.87	189.7
264.75	654.7	177.07	505.4	17.57	27.37	54.89	195.0
267.05	657.9	179.26	508.4	18.81	31.45	55.91	199.9
269.35	660.7	181.47	512.7	20.05	35.52	56.94	205.6
271.66	664.7	183.69	516.7	21.27	39.77	57.96	211.0
273.98	668.0	185.91	520.9	22.51	44.35	58.99	216.5
276.31	670.7	188.15	525.1	23.77	49.00	60.02	221.7
278.64	673.8	190.39	529.2	25.03	53.70	61.06	225.1
280.98	677.4	192.64	533.4	26.28	58.52	62.11	224.9
283.32	680.1	194.91	536.9	27.52	64.45	63.16	226.8
285.67	683.4	197.18	541.2	28.75	69.57	64.22	229.7
288.03	685.9	199.46	544.7	29.96	74.75	65.28	231.5
290.39	689.0			31.16	80.27	66.35	235.2
292.75	692.5			32.34	85.89	67.42	238.7
295.13	696.5	13.06	14.19	33.50	91.09	68.50	241.6
297.52	699.5	14.12	16.94	34.64	96.36	69.59	245.0
299.91	703.2	15.15	19.75	35.79	100.9	70.68	247.9
		16.15	22.76	36.95	107.6	71.77	252.8
		17.15	25.79	38.19	114.0	72.87	254.9
79.03	272.8	18.13	28.92	39.50	120.8	73.97	257.8
81.09	279.6	19.11	32.21	40.88	127.4	75.08	259.8
83.13	285.9	20.08	35.63	42.30	134.5	76.19	264.4
85.15	291.3	21.03	39.08	43.70	141.3	77.31	269.0
87.17	297.0	22.01	42.54	45.15	147.6	78.43	273.5
89.17	302.4	23.03	46.14	46.65	154.5	79.56	274.7
91.16	308.0	24.07	49.83	48.11	161.9		
93.15	313.8	25.12	53.94	49.56	168.6		
95.13	318.9	26.17	58.04	50.98	175.6		
97.11	324.2	27.22	62.40	52.38	182.4		
99.09	329.6	28.27	67.04	53.77	189.3		
101.06	335.0	29.31	71.71	55.15	196.5		
103.03	339.8	30.34	76.20	56.51	203.1		

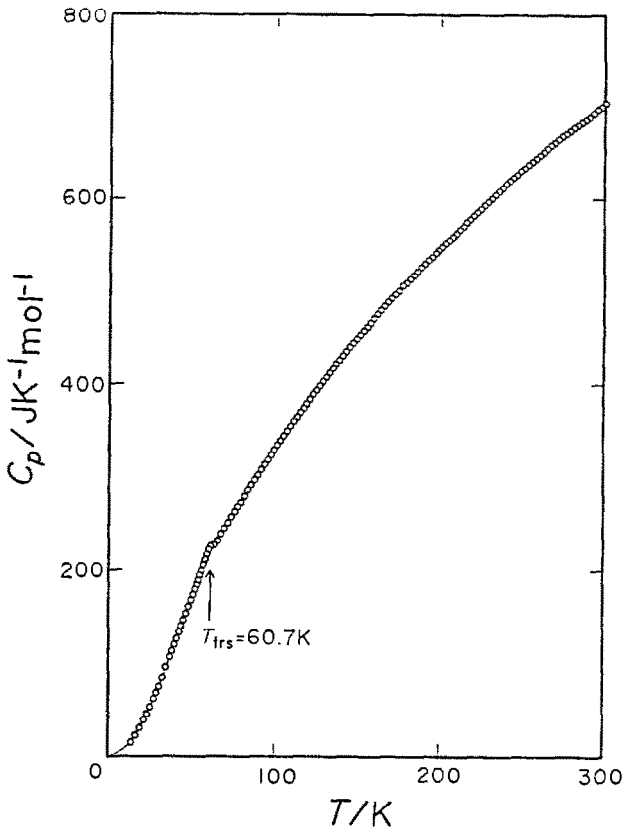

Fig. 1. Molar heat capacity of the manganese squarate clathrate compound.

peak due to a latent heat and the gradual increase of the heat capacity below the transition temperature) suggested that the compound underwent a higher order phase transition. The observed heat capacity was assumed to consist additively of the normal and transitional parts. The normal heat capacity was determined as follows. The contribution of the lattice vibration to the heat capacity was represented by a sum of the Debye and Einstein functions. All of the normal modes of vibrations of squarate, acetic acid, and water molecules have been identified in infrared and Raman spectra (refs. 5-7). They were used in the calculation of the normal heat capacity. The unknown part consists of the translational and librational lattice vibrations and was expressed as a sum of the Debye and Einstein heat capacity functions. The unknown Debye and Einstein temperatures were determined by the least squares fitting of the heat capacity data in the temperature ranges from 12 to 35 K and from 80 to 130 K

where it could safely be assumed that the effect of the phase transition was negligibly small. The transition enthalpy and entropy, determined as the integrals $\int \Delta C_p \, dT$ and $\int \Delta C_p / T \, dT$ of the excess contribution over the normal heat capacity, were 120 J mol^{-1} and 2.13 J $K^{-1}mol^{-1}$, respectively.

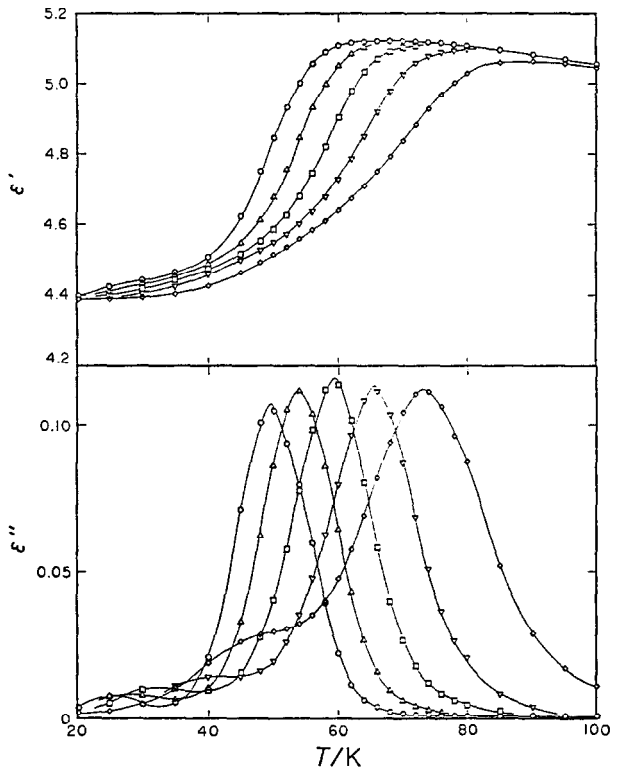

Fig. 2. Complex dielectric permittivity of the manganese squarate clathrate compound. Upper: real part, lower: imaginary part. ○: 100 Hz, △: 1 kHz, □: 10 kHz, ▽: 100 kHz, ◇: 1 MHz.

The complex dielectric permittivity of the compound is plotted in Fig. 2 as a function of temperature. Two dielectric dispersions occurred, of which the one observed at higher temperature was more pronounced than the other. Magnitude of each dispersion depended on the temperature (and thus on the frequency) in distinct ways. The lower-temperature dispersion decreased in its magnitude as the temperature (and thus the frequency) is lowered. Since the two dispersions were symmetrical and broader than the normal Debye type behavior, attempt was made to fit the Cole-Cole equation to the experimental data (ref. 8). Three parameters were involved:

$$\varepsilon = \varepsilon_\infty + \frac{\varepsilon_0 - \varepsilon_\infty}{1 + (i\omega\tau)^{1-\alpha}}.$$

The values of α were in the range between 0.2 and 0.6. This indicates moderate departure from the single relaxation kinetics of the process. The tendency of the decrease of α with rising temperature (e.g. α = 0.52 at 50 K and α = 0.37 at 70 K in the higher-temperature dispersion) was also observed in other clathrate compounds such as hydroquinone clathrate compounds (ref. 9). The activation enthalpy of the lower- and higher-temperature dispersions were determined to be 4.01 and 11.5 kJ mol^{-1}, respectively.

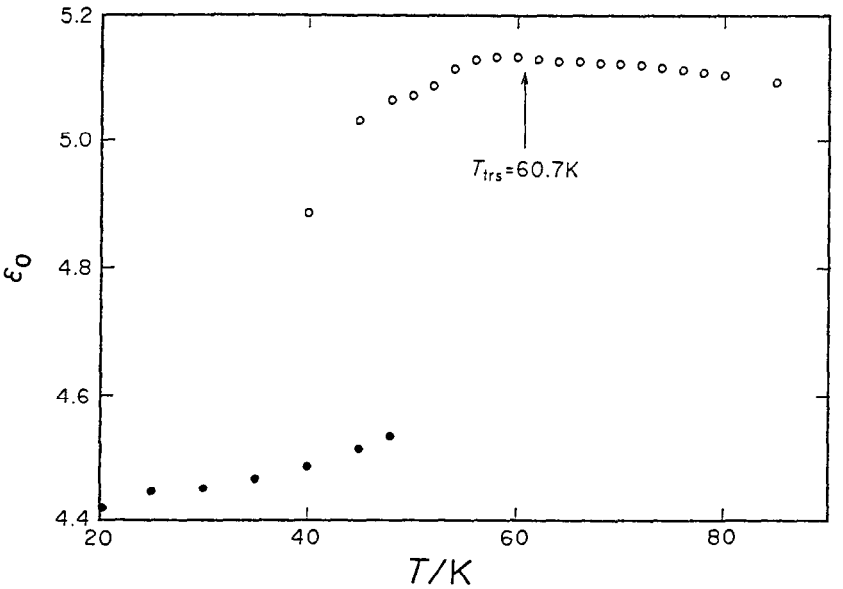

Fig. 3. Static dielectric permittivity of the manganese squarate clathrate compound. O: higher-temperature dispersion, ●: lower-temperature dispersion.

The two dielectric dispersions in the present compound indicate that there are two different motional modes. They are most likely to have been caused by the motion of the guest molecules since the host lattice forms a rigid framework and the guest molecules are heavily disordered (ref. 2). Several possible models of molecular motion to be connected with the two dispersions can be considered. There are two kinds of guest molecules, the water and acetic acid. Since both are polar, they may be responsible for the two dispersions separately. It is also possible that only one of them is actually involved in the two

dispersions, two time constants being connected with different axes of rotation. As the third possibility, one may invoke hydrogen-bonded pairs occupying some cavities and monomers (water or acetic acid) occupying others. They would cause separate dispersions because of the different ease of reorientational motion they have in the cavity. Experimental distinction among these possibilities may be made by studying the clathrate compounds of different stoichiometry.

The static dielectric permittivity of the compound is plotted against temperature in Fig. 3. The higher order phase transition at 60.7 K is probably related to the ordering of the guest molecules in view of the change of slope of the static permittivity at the temperature, as shown in Fig. 3 (ref. 10). The negative slope for $T > T_c$ is the usual Curie-Weiss behavior. For $T < T_c$, the number of the guest molecules that respond to the external field decreases as the ordering proceeds with the falling temperature. This causes gradual decrease of the static dielectric permittivity as was actually observed.

In this work, the identification of the motional modes of the guest molecules could not be made. X-ray study of crystal structure of the present compound below the transition temperature is evidently desirable.

CONCLUSION

Two dielectric dispersions occurred at low temperatures in the manganese squarate clathrate compound. The dielectric absorption peaks were broader than the Debye dispersion and reproduced well by the Cole-Cole functional form. There are thus two distinct molecular motions. In view of the rigidity of the host lattice, the two dispersions may be related to the guest molecules. But more specific identification could not been made. The compound underwent a higher order phase transition at 60.7 K. The static dielectric permittivity of the compound changed its slope at $\sim$60 K as the temperature is traversed. This agrees with the calorimetric result and may be related to ordering of the polar guest molecules.

REFERENCES

1 A. Weiss, E. Riegler, and C. Robl, Z. Naturforsch. **41b** (1986) 1329.
2 A. Weiss, E. Riegler, and C. Robl, Z. Naturforsch. **41b** (1986) 1333.
3 Y. Ogata, K. Kobayashi, T. Matsuo, and H. Suga, J. Phys. E **17** (1984) 1054.
4 T. Matsuo and H. Suga, Solid State Commun. **21** (1977) 923.
5 M. Ito and R. West, J. Am. Chem. Soc. **85** (1963) 2580.
6 M. Haurie and A. Novak, Spectrochim. Acta **21** (1965) 1217.
7 D. Eisenberg and W. Kauzmann, The Structure and Properties of Water, Chapter 3, Oxford University Press (1969).

8 K. S. Cole and R. H. Cole, J. Chem. Phys. **9** (1941) 341.
9 J. A. Ripmeester, R. E. Hawkins, and D. W. Davidson, J. Chem. Phys. **71** (1979) 1889.
10 H. Fröhlich, Theory of Dielectrics, Oxford University Press (1958).